Available online at www.sciencedirect.com
SCIENCE DIRECT®
Journal of Nuclear Materials 337–339 (2005) 732–736
journal of nuclear materials
www.elsevier.com/locate/jnucmat

Integrated exhaust control with divertor parameter feedback and pellet ELM pacemaking in ASDEX Upgrade

A. Kallenbach *, P.T. Lang, R. Dux, C. Fuchs, A. Herrmann, H. Meister, V. Mertens, R. Neu, T. Pütterich, T. Zehetbauer, the ASDEX Upgrade Team

Max-Planck-Institut für Plasmaphysik, IPP – EURATOM Association, Boltzmannstr. 2, D-85748 Garching b.München, Germany

Abstract

An integrated exhaust scenario has been developed in ASDEX Upgrade providing simultaneous control of particle exhaust, time averaged divertor power flux and ELM power via pace-making of the ELM frequency. Feedback quantities are the divertor neutral flux (actuator: deuterium gas puff) and the divertor temperature as measured by thermoelectric currents (actuator: argon gas puff). The ELM frequency is stabilised to a level high enough for moderate ELM power load with repetitive injection of small pellets from the high field side. The scenario is fully compatible with the present tungsten wall coating, which constitutes about 65% of the area of the plasma facing components. It is intended for application in a future full-tungsten ASDEX Upgrade with strongly reduced intrinsic carbon radiation in order to simulate a possible full-tungsten stage of ITER.

PACS: 52.55.Fa; 52.25.Vy; 52.55.Rk; 52.40.Hf
Keywords: ASDEX Upgrade; Edge plasma; Heat flux; Impurity; ELM

1. Introduction

The development of integrated scenarios for power and particle exhaust in type-I ELMy H-modes for ITER requires the inclusion of active control of the ELM power. This can be achieved by increasing the ELM frequency by active pace-making taking advantage of the inverse relation of ELM frequency and power load [1].

A high performance scenario for simultaneous feedback control of the divertor neutral flux (particle exhaust rate) and the divertor temperature (inter-ELM power load) using impurity injection in combination with pellet ELM-pacemaking has been recently developed at ASDEX Upgrade. The scenario aims at integrated power and particle exhaust in a carbon-free, full-tungsten tokamak. With seed impurities like Ne or Ar, radiative power exhaust takes place predominantly in a radiative mantle around the main plasma surface [2,3]. As a consequence, the H-mode working point is situated close to the H–L power threshold, with low natural type-I ELM frequency. A low type-I ELM frequency is often connected to strong impurity influx and may cause a radiation-driven H–L backtransition, as will be shown below. The ELM frequency can be kept at a sufficiently high level by repetitive injection of small cryogenic pellets, resulting in a low central impurity level

* Corresponding author. Tel.: +49 89 3299 1721; fax: +49 89 3299 1812.
E-mail address: arne.kallenbach@ipp.mpg.de (A. Kallenbach).

0022-3115/$ - see front matter © 2004 Elsevier B.V. All rights reserved.
doi:10.1016/j.jnucmat.2004.10.027

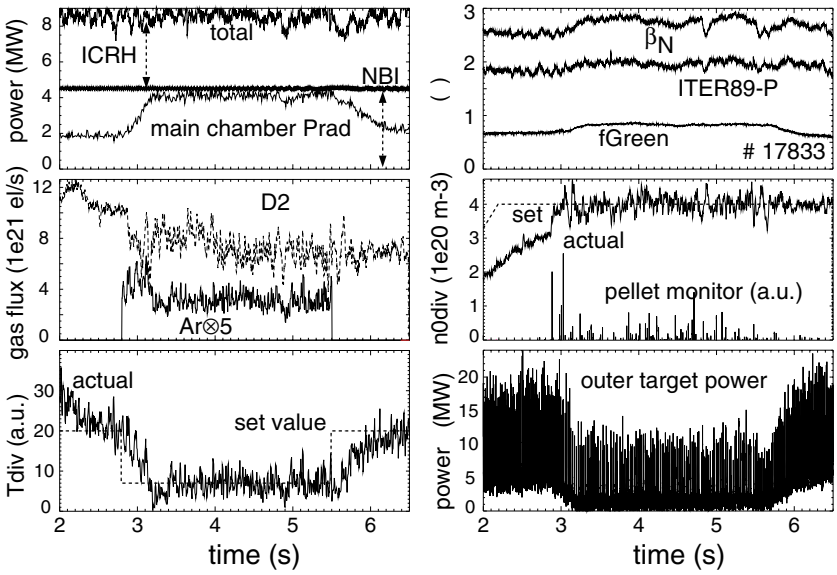

Fig. 1. Time traces of a discharge with simultaneous feedback of the divertor neutral flux and the divertor temperature while the ELM frequency is stabilized by repetitive pellet injection at 41 hz. β_N denotes the normalised plasma pressure, ITER89-P the confinement time relative to the ITER89-P L-mode scaling and f_{Green} the ratio of line-averaged and Greenwald density, which corresponds to $\bar{n}_e = 1.2\,10^{20}\,m^{-3}$ here. $I_p = 1\,MA$, $B_t = -2\,T$, $q_{95} = 4.0$, $\delta = 0.3$.

while good confinement is maintained. Fig. 1 shows time traces of a discharge with integrated exhaust control, corresponding divertor parameters are shown in Fig. 2.

A mix of neutral beam injection and central ICRH is used to ensure sufficient central power flow to avoid central density peaking and possible subsequent tungsten accumulation [4]. The density profiles during the cooling phase remain flat, as shown in Fig. 3 for the discharge of Fig. 1. This is essential to allow for moderate values of Z_{eff} and tungsten concentrations. The central Ar content is derived form H- an He-like Ar lines measured by a Bragg crystal spectrometer and subsequent modelling with the impurity transport code STRAHL [5]. The central Ar concentration is about 0.18%, corresponding to a ΔZ_{eff} of 0.5, with an uncertainty of a factor of 2 caused by the absolute calibration and the atomic data. Notably, a significant increase in the pedestal density during the radiative cooling phase is observed. This density rise allows for an increased radiation level while keeping the total Z_{eff} about constant.

2. Feedback system for power and particle exhaust

The 'effective' divertor temperature is obtained from online measurements of the thermoelectric currents

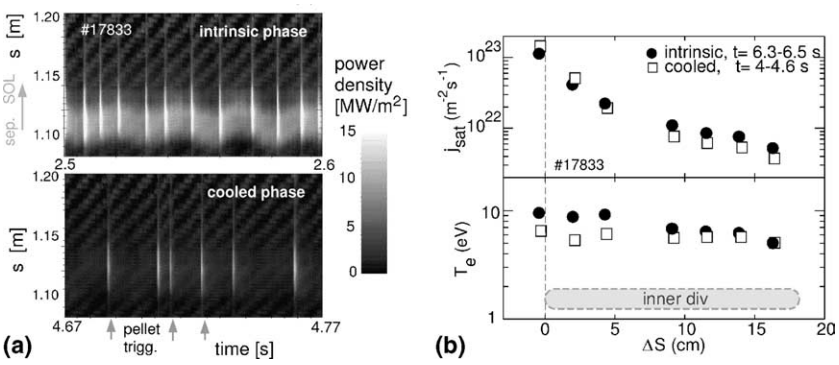

Fig. 2. (a) Heat flux at the lower outer target during the intrinsic phase and during feedback controlled cooling for the discharge shown in Fig. 1. (b) shows profiles of ion saturation current and electron temperatures from Langmuir probes. Much lower electron temperatures are observed in the inner divertor.

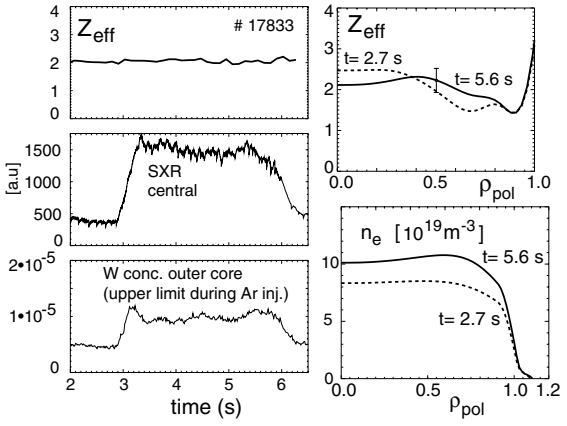

Fig. 3. Line averaged Z_{eff} from visible bremsstrahlung deconvolution, central soft-X radiation and tungsten concentration evaluated from the W quasi-continuum. Z_{eff} profiles and density profiles from combined Li-beam and DCN interferometer deconvolution are shown on the right hand side for times just before and at the end of the Ar injection.

flowing between the inner and outer divertor [6], which are a measure for the difference of the divertor temperatures and also represent the power load. The net currents are caused via thermoelectric effects by the temperature difference between the two SOL ends [7]. The scheme works for fully and partially attached conditions, the thermoelectric current vanishes during detachment. Feedback actuators are D_2 and Ar gas fuelling through valves situated at the outer midplane. The pellet frequency is preset, operation of the centrifuge allows injection frequencies of $250/n$ Hz, with $n \geqslant 3$ [1]. The neutral deuterium flux density is measured by an ionisation gauge below the roof baffle. This flux is directly proportional to the pumped particle flux. A prerequisite for feedback controlled cooling is a sufficiently fast removal rate. The decay time of the edge Ar recycling after the valve is closed has been measured by a SPRED VUV spectrometer to be around 0.3 s, demonstrating good Ar divertor compression and pumping.

3. Impurity behaviour

A burning fusion reactor is expected to require a high-Z (probably tungsten) wall and divertor since only very low erosion and tritium codeposition rates will be acceptable. ASDEX Upgrade is being converted to a full-tungsten tokamak within the next couple of years, with presently about 65% of the plasma facing components coated with tungsten [4]. The integrated exhaust scenario has to compensate the accompanying reduction of the intrinsic carbon radiation and must be compatible with the presence of large tungsten wall areas. Former radiative cooling scenarios in ASDEX Upgrade were based on benign type-III ELMs (CDH-Mode) [8], where central density profile peaking partly compensated for the confinement loss connected to the reduction in pedestal pressure. Such a pronounced central peaking is expected to be incompatible with the presence of large tungsten walls.

The combination of high-Z wall and radiative cooling is an issue since sputtering by medium-Z ions is the dominant erosion mechanism [9]. Generally, the sputtering yield for a given impact energy rises with impinging ion mass. In contrast, the plasma seed impurity concentration decreases with mass in a realistic scenario, since the main plasma $\Delta P_{\text{rad}}/\Delta Z_{\text{eff}}$ rises with the impurity charge [10]. Fig. 4 shows tungsten sputtering yields, multiplied by their estimated concentration for D, He, C, Ne, Ar and Kr as a function of edge temperature, assuming $E_{\text{impact}} = 3ZT + 2T$. By multiplication with the impurity concentrations, the sputtering yields refer to the impinging D flux and realistic relative fractions of W release are obtained. Fig. 4 suggests no pronounced variation of the total W sputtering for different radiating species, in particular Ne, Ar and Kr give very similar effective yields.

The experimental observations for discharges similar to that shown in Fig. 1 are as following: The tungsten influx from a low field side limiter as measured by visible spectroscopy [9] remains about constant during the Ar seed phase, while the tungsten concentration rises slightly. The carbon and hydrogen main chamber fluxes decrease slightly, while the power flow into the divertor is significantly reduced (by 2 MW in the case shown in Fig. 1). As a consequence, the divertor radiation measured by bolometry is reduced as well, in line with an

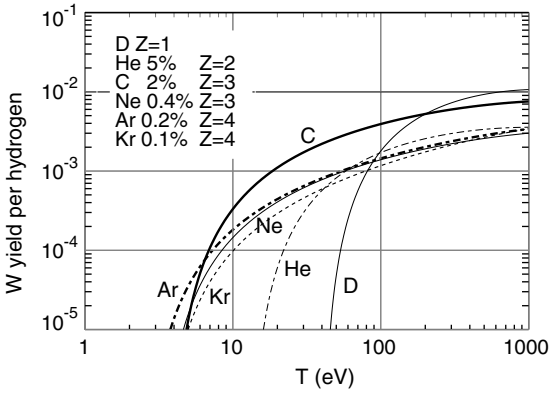

Fig. 4. Tungsten sputtering yields taken from [11] for different species versus plasma temperature, assuming an impact energy $E = 3ZT + 2T$. Total yields are multiplied by the assumed concentrations to obtain realistic, effective yields per fuel ion flux. Charge states used for the calculation are given in the inset.

earlier observation that the divertor radiation is mainly proportional to the power flux into the divertor [12]. Analysis of CII and CIII spectral lines indicates a reduced carbon sputtering in the divertor during the Ar seed phase, while Ar itself does not contribute significantly to divertor radiation due to the temperature dependence of its radiative loss function.

The increased electron density during the Ar seed phase is related to an improved particle confinement time, since the neutral deuterium divertor flux is feedback controlled to a constant value. This is also in line with the observation of a constant core carbon density despite reduced sources. Among the possible explanations for the enhanced particle confinement are reduced ELM particle losses and an improved core penetration probability for neutrals due to reduced edge temperatures.

4. Importance of ELM frequency control

The general benefit of ELM pacemaking is the reduction of the ELM power with increasing frequency, which is valid for triggered as well as intrinsic ELMs [1]. As shown in Fig. 2(a) and observed in other experiments [13,3], the type-I ELM frequency is reduced during radiative cooling due to the reduced power flow over the edge transport barrier (ETB) region. Despite the frequency reduction the ELM energy is also reduced compared to the non-seeded phase. This is probably due to the increased collisionality in the pedestal region [14] at increased density and reduced temperature. In DIII-D it was shown that the conducted fraction of the ELM energy decreases with rising pedestal density, while the convected fraction remains about constant [15]. However, a too low ELM frequency may cause the development of a radiative instability, as shown in Fig. 5. The instability is assumed to be caused by the reduction of the type-I ELM frequency with decreasing power flux through the ETB [16]: In between ELMs, the plasma radiation rises strongly. The resulting reduced power flux through the ETB further delays the next ELM. Finally, the radiation rises to a level where a H–L backtransition occurs. The divertor plasma detaches immediately, the effective T_{div} derived from thermocurrents goes to zero and the feedback system reacts with a closure of the Ar valve. Stable H-mode operation is reached again after typically 0.2 s. The non-linear response of the thermoelectric signal, which is more pronounced than T_e from a Langmuir probe, is very helpful to cure such radiative instabilities and to feedback on semi-attached conditions. However, the reaction time based mainly on the feedback gain and the speed of the Ar valve is too slow for fully steady (semi-)attached H-mode operation, for which ELM pacemaking is necessary.

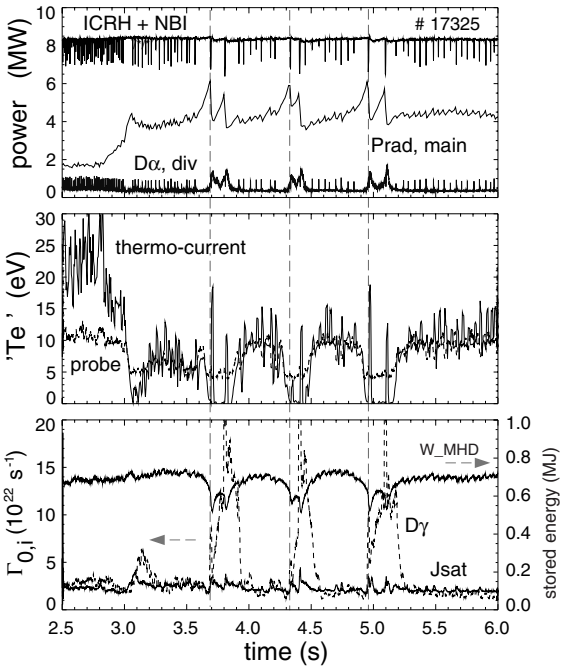

Fig. 5. Time traces for a Ar cooled discharge without pellet ELM pacemaking showing 3 short phases of radiative instabilities. Top: heating power, main chamber radiation and D_α ELM monitor. Middle: T_e from Langmuir probe 4 cm above separatrix. Bottom: stored energy, Jsat and neutral flux from D_γ 4 cm above separatrix using S/XB values derived from the probe data. During the phases with reduced confinement, the D influx derived from D_γ emission exceeds the ion flux indicating recombination.

5. Discussion and conclusions

We have developed an integrated particle and power exhaust feedback scenario aiming towards a full-tungsten wall, carbon-free tokamak. A considerable fraction of central heating is used to avoid central impurity peaking. Ar seeding is used to control the power flux over the separatrix, while deuterium puffing is used to control the neutral flux density in the divertor, which determines the plasma density, the power exhaust in the divertor and the gas removal rate through the pump. As a consequence of the electron temperature dependence of the radiative loss function of medium-Z noble gases, active radiation control of power exhaust means operation close to the H–L transition, since the radiative power removal takes place in the separatrix/pedestal region. The operation near the H–L threshold may cause large, low frequency type-I ELMs with negative implications for the target lifetime [17] and central radiation levels. The use of the thermocurrents for the power exhaust control turned out to be particularly useful under these conditions of low power flux into the divertor. Their non-linear characteristic at low temperatures helps to avoid or

cure conditions of a recombining outer divertor plasma, which is closely connected to pedestal and core confinement degradation. Active ELM triggering by injection of small pellets avoids unstable situations with excursions of the radiation and allows for steady operation. It should be noted that the artificial elevation of the ELM frequency has to be generally foreseen in an integrated scenario with type-I ELMs, since the expected natural ELM frequency in ITER is too low [18]. The artificial rise of the ELM frequency leads to lower ELM energies at a moderate price in terms of confinement loss. These beneficial effects need to be further quantified and understood to allow for a scaling towards reactor conditions.

References

[1] P. Lang et al., Nucl. Fusion 44 (2004) 665.
[2] A. Kallenbach et al., Plasma Phys. Control. Fusion 38 (1996) 2097.
[3] G. Maddison et al., Nucl. Fusion 43 (2003) 49.
[4] R. Neu et al., J. Nucl. Mater. 313–316 (2003) 116.
[5] R. Dux et al., Nucl. Fusion 39 (1999) 1509.
[6] A. Kallenbach et al., J. Nucl. Mater. 290–293 (2001) 639.
[7] G.M. Staebler, F.L. Hinton, Nucl. Fusion 29 (1989) 1820.
[8] A. Kallenbach et al., Nucl. Fusion 35 (1995) 1231.
[9] R. Dux et al., these Proceedings.
[10] A. Kallenbach et al., Fusion Eng. Des. 36 (1997) 101.
[11] W. Eckstein et al., Report IPP 9/82, IPP Garching, 1993.
[12] A. Kallenbach et al., Nucl. Fusion 39 (1999) 901.
[13] S. Higashijima et al., J. Nucl. Mater. 313–316 (2003) 1123.
[14] A. Loarte et al., J. Nucl. Mater. 313–316 (2003) 962.
[15] A. Leonard, J. Boedo, M. Fenstermacher, et al., J. Nucl. Mater. 313–316 (2003) 768.
[16] H. Zohm, Plasma Phys. Control. Fusion 38 (1996) 105.
[17] F. Federici et al., Plasma Phys. Control. Fusion 45 (2003) 1523.
[18] A.R. Polevoi et al., Nucl. Fusion 43 (2003) 1072.